SVN Stroke & Vascular Neurology

Bone marrow-derived mesenchymal stem cell ameliorates post-stroke enterobacterial translocation through liver-gut axis

Xiaotao Su,[1,2,3] Tiemei Li,[1] Yuge Wang,[1] Lei Wei,[1] Banghao Jian,[1] Xinmei Kang,[1] Mengyan Hu,[1] Chunyi Li,[1] Shisi Wang,[1] Danli Lu,[1] Shishi Shen,[1] Huipeng Huang,[1] Yuxin Liu,[1] Xiaohui Deng,[1] Bingjun Zhang,[1] Wei Cai ,[1,2,3] Zhengqi Lu [1]

To cite: Su X, Li T, Wang Y, *et al*. Bone marrow-derived mesenchymal stem cell ameliorates post-stroke enterobacterial translocation through liver-gut axis. *Stroke & Vascular Neurology* 2024;**0**. doi:10.1136/svn-2024-003494

► Additional supplemental material is published online only. To view, please visit the journal online (https://doi.org/10.1136/svn-2024-003494).

XS and TL contributed equally.

Received 20 June 2024
Accepted 4 September 2024

[1]Department of Neurology, Mental and Neurological Disease Research Center, The Third Affiliated Hospital of Sun Yat-Sen University, Guangzhou, Guangdong, China
[2]Center of Clinical Immunology, Mental and Neurological Disease Research Center, The Third Affiliated Hospital of Sun Yat-Sen University, Guangzhou, Guangdong, China
[3]Guangdong Provincial Key Laboratory of Brain Function and Disease, Guangzhou, Guangdong, China

Correspondence to
Dr Zhengqi Lu;
luzhq@mail.sysu.edu.cn

Dr Wei Cai;
caiw29@mail.sysu.edu.cn

Dr Bingjun Zhang;
zhangbj5@mail.sysu.edu.cn

ABSTRACT

Background Enterobacterial translocation is a leading contributor to fatal infection among patients with acute ischaemic stroke (AIS). Accumulative evidence suggests that mesenchymal stem cell (MSC) effectively ameliorates stroke outcomes. Whether MSC could inhibit post-stroke enterobacterial translocation remains elusive.

Methods Patients with AIS and healthy individuals were enrolled in the study. Mice subjected to transient middle cerebral artery occlusion were treated with bone marrow-derived MSC (BM-MSC) right after reperfusion. Enterobacterial translocation was evaluated with Stroke Dysbiosis Index and circulating endotoxin. Thickness of mucus was assessed with Alcian blue staining. Hepatic glucocorticoid (GC) metabolism was analysed with expression of HSD11B2, HSD11B1 and SRD5A1.

Results We report that the gut mucus layer was attenuated after the stroke leading to pronounced enterobacterial translocation. The attenuation of the gut mucus was attributed to diminished mucin production by goblet cells in response to the elevated systemic GC after cerebral ischaemia. Transferred-BM-MSC restored the mucus thickness, thus preserving gut microbiota homeostasis and preventing enterobacterial invasion. Mechanistically, the transferred-BM-MSC stationed in the liver and enhanced peroxisome proliferator-activated receptor γ signalling in hepatocytes. Consequently, expression of HSD11B2 and SRD5A1 was increased while HSD11B1 expression was downregulated which promoted GC catabolism and subsequently restored mucin production.

Conclusions Our findings reveal that MSC transfer improves post-stroke gut barrier integrity and inhibits enterobacterial translocation by enhancing the hepatic GC metabolism thus representing a protective modulator of the liver-gut-brain axis in AIS.

WHAT IS ALREADY KNOWN ON THIS TOPIC

⇒ Acute ischaemic stroke (AIS) is a serious global health burden. Enterobacterial translocation mediates post-stroke infection and is thus a leading contributor to the mortality of AIS which may be a promising target.
⇒ Accumulative evidence suggests that bone marrow-derived mesenchymal stem cell (BM-MSC) effectively improves stroke outcomes and protect against infectious diseases.

WHAT THIS STUDY ADDS

⇒ Thickness of the gut mucus layer is attenuated after stroke. BM-MSC transfer restores the mucus thickness and subsequently inhibits enterobacterial translocation.
⇒ Systemic elevation of glucocorticoid (GC) after stroke inhibits mucin production by gut goblet cells which is reversed by BM-MSC treatment.
⇒ The transferred-BM-MSC is largely stationed in the liver but hardly infiltrates into the gut. The curative effects of BM-MSC are attributed to the enhanced GC catabolism in hepatocytes.
⇒ Mechanistically, BM-MSC activates peroxisome proliferator-activated receptor γ signalling in hepatocytes leading to increased GC catabolism which inhibits the injurious effect of GC on gut barrier integrity.

HOW THIS STUDY MIGHT AFFECT RESEARCH, PRACTICE OR POLICY

⇒ Mucus layer attenuation facilitates enterobacterial translocation after stroke. To preserve mucus thickness and to enhance mucin production by gut goblet cells represent promising preventive strategies against enterobacterial translocation and post-stroke infection.
⇒ Liver-gut-brain axis affects stroke prognosis. BM-MSC improves stroke outcomes through modulating the liver-gut axis.

INTRODUCTION

Acute ischaemic stroke (AIS) is one of the leading causes of death worldwide.[1] Accumulative evidence reveals the dysbiosis of gut microbiota in patients with AIS and the subsequent detrimental impacts on stroke outcomes.[2 3] Translocation of enterobacteria and the consequent systemic infection exacerbate neurological dysfunction and worsen stroke prognosis.[4 5] Therefore, inhibition of enterobacteria translocation is regarded as a promising therapeutic strategy in AIS.

Despite the evident translocation of enterobacteria, gut serosal, muscular and submucous layers remain to be intact in stroke models after cerebral ischaemia.[6] The mucus layer, which consists of mucin produced by goblet cells, represents a non-structural barrier in

the gut that precludes pathogen invasion.[7] Nevertheless, alteration of the gut mucus after stroke remains elusive.

Mesenchymal stem cell (MSC) has been shown to effectively ameliorate stroke outcomes in several studies.[8 9] Recent research reveals that the transfer of MSC modulates the composition of gut microbiota.[10–12] Therapeutic benefits of MSC transfer against post-stroke infection have been documented.[13] Nevertheless, the impacts of MSC treatment on enterobacterial translocation are to be investigated. On the other hand, intravenously transferred MSC hardly infiltrated into the gut. The underlying mechanisms of how MSC modulates gut activities and the homeostasis of gut microbiota are questions to be answered.

The current study explores the therapeutic effects of bone marrow-derived MSC (BM-MSC) against post-stroke enterobacterial translocation. We found that the thickness of the gut mucus layer was attenuated after stroke which permitted the translocation of gut bacteria. Mechanistically, systemic elevation of glucocorticoid (GC) in response to cerebral ischaemia suppresses mucin production by gut goblet cells. BM-MSC transfer accelerates GC degradation in the liver thus preserving mucin production. As a result, attenuation of the mucus layer is reversed in BM-MSC recipients and the subsequent enterobacterial translocation is forbidden. We thus propose that BM-MSC transfer is a promising therapy against post-stroke enterobacterial translocation through regulating the liver-gut axis.

MATERIALS AND METHODS

Human samples

The cohort consisted of 74 patients with AIS, 40 age-matched and sex-matched healthy controls. Patient demographics were summarised in online supplemental table 1. Samples of patients with AIS were collected within 0–7 days after stroke onset. Plasma samples were obtained by centrifuging peripheral blood at 15 000 g for 15 min at 4°C. Genomic DNA protective solution (Longsee, LS-R-P-003) was used to collect fresh faecal samples donated by recruited patients.

Animals

Wild-type (WT) C57/BL6 mice were purchased from Guangdong Medical Laboratory Animal Center (Guangzhou, China) and were kept in a facility with controlled temperature and humidity. For the in vivo experiments, mice aged 8–10 weeks with a body weight of 18–25 g were used.

Cells

Human BM-MSC was obtained as previously described.[14] Briefly, a density gradient centrifugation method using Ficoll-Paque (17-1440-02, GE) was used to isolate BM-MSC from bone marrow. The separated BM-MSC were cultured in an MSC medium (GIBCO, A13829-01 and A11577-01). Details of BM-MSC identification were indicated in Expanded methods in online supplemental material. MC38 and HEK293T cells were obtained from American Type Culture Collection. MC38 was used as a goblet cell and was cultured in RPMI1640 medium (GIBCO, C11875500BT) with 10% fetal bovine serum (FBS) and 1% P/S. HEK293T was cultured in a Dulbecco's Modified Eagle's Medium-high glucose medium (GIBCO, C11995500BT) with 10% FBS and 1% P/S. Primary hepatocytes were obtained by employing a two-stage perfusion technique.[15] Livers digested with collagenase IV (100 U/mL; Sigma-Aldrich, C5138) were washed by centrifugation at 50 g for 1 min at 4°C. Resuspended used Williams' Medium E (GIBCO, 12551032) with 10% FBS and 2% P/S, the hepatocytes were seeded on type I rat tail collagen-coated culture plates (Invitrogen, A048301) and incubated at 37°C. The medium was refreshed at 2 hours after incubation. Hepatocytes were changed to serum-free medium 6 hours later and used for experiments on the following day. Details about the experimental procedure are given in the Expanded methods in online supplemental material.

Murine acute cerebral ischaemic stroke models

As described previously, a transient middle cerebral artery occlusion model (tMCAO) was used to induce an AIS.[16] Mice were anaesthetised with 5% isoflurane and were maintained with 1.5% isoflurane. Then, a silicone rubber-covered monofilament matching the body weight of the mouse (weight: 15–20 g, diameter: 0.19±0.01 mm; weight: 20–25 g, diameter: 0.21±0.01 mm) was inserted into the internal carotid artery through the external carotid artery. The monofilament was retracted after 60 min later for brain reperfusion. The model group recruited mice with 70% or more regional cerebral blood flow reduction under laser speckle blood flow imager (SIM BFI HR Pro, SIM Opto-Technology Co., Ltd) monitoring and randomly assigned them to the treatment group. Mice that died or developed subarachnoid haemorrhage were excluded. The sham group experienced the same operation except that the monofilament was not inserted. Assessment of neurological function and infarct volume were indicated in Expanded methods in online supplemental material.

Treatments of mice

For BM-MSC transplantation, 2×10^6 cells (5–8 passages) were suspended in 0.1 mL phosphate-buffered saline and transplanted via the inner canthal orbital vein right after reperfusion. Mice in the Veh group were injected intraperitoneally with equal amounts of vehicle. For the broad-spectrum antibiotics (ABX) experiment, the drinking water of mice was replaced with an ABX cocktail for 28 days to deprive the intestinal microbiota until tMCAO was conducted. To prepare the ABX cocktail, ampicillin (1 g/L, Macklin, A830931), metronidazole (1 g/L, Macklin, M813526), neomycin (1 g/L, Macklin, N6063) and vancomycin (0.5 g/L, Macklin, V871983) were dissolved in autoclaved water. In the GC therapy experiment, mice in the dexamethasone (DEX) group were

injected with DEX (0.25 mg/kg, intraperitoneally (i.p)) at 2 hours after reperfusion while mice in the DEX+MSC group received DEX (0.25 mg/kg, i.p) in addition to BM-MSC transplantation. Details of experimental procedures were provided in the Expanded methods in online supplemental material.

Statistical analysis

GraphPad Prism software (V.9.5) was used for statistical analysis. Data were presented as the mean and error bars represent SD. Student's t-test or Welch's t-test was used to compare data between two groups, as appropriate. For multiple comparisons, differences were evaluated by using one-way or two-way analysis of variance (ANOVA) or Welch ANOVA followed by Tukey's multiple comparison test or Dunnett's multiple comparison test. The association between indicators was assessed through Spearman's correlation analysis. The analysis of survival data was conducted using Kaplan-Meier survival curves followed by a comparison with a log-rank test. Differences with p values <0.05 were considered significant.

RESULTS

BM-MSC transfer ameliorates post-stroke enterobacterial translocation

In consistent with previous reports, we recorded gut bacteria translocation in patients with AIS (figure 1A) as revealed by increased concentration of plasma lipopolysaccharides (LPS, figure 1B) and LPS binding protein (LBP, figure 1C). In the meantime, the Stroke Dysbiosis Index[17] (SDI, online supplemental figure 1A–C) which revealed the disorder of gut microbiota was increased in the recruited patients with AIS (figure 1D). Notably, SDI

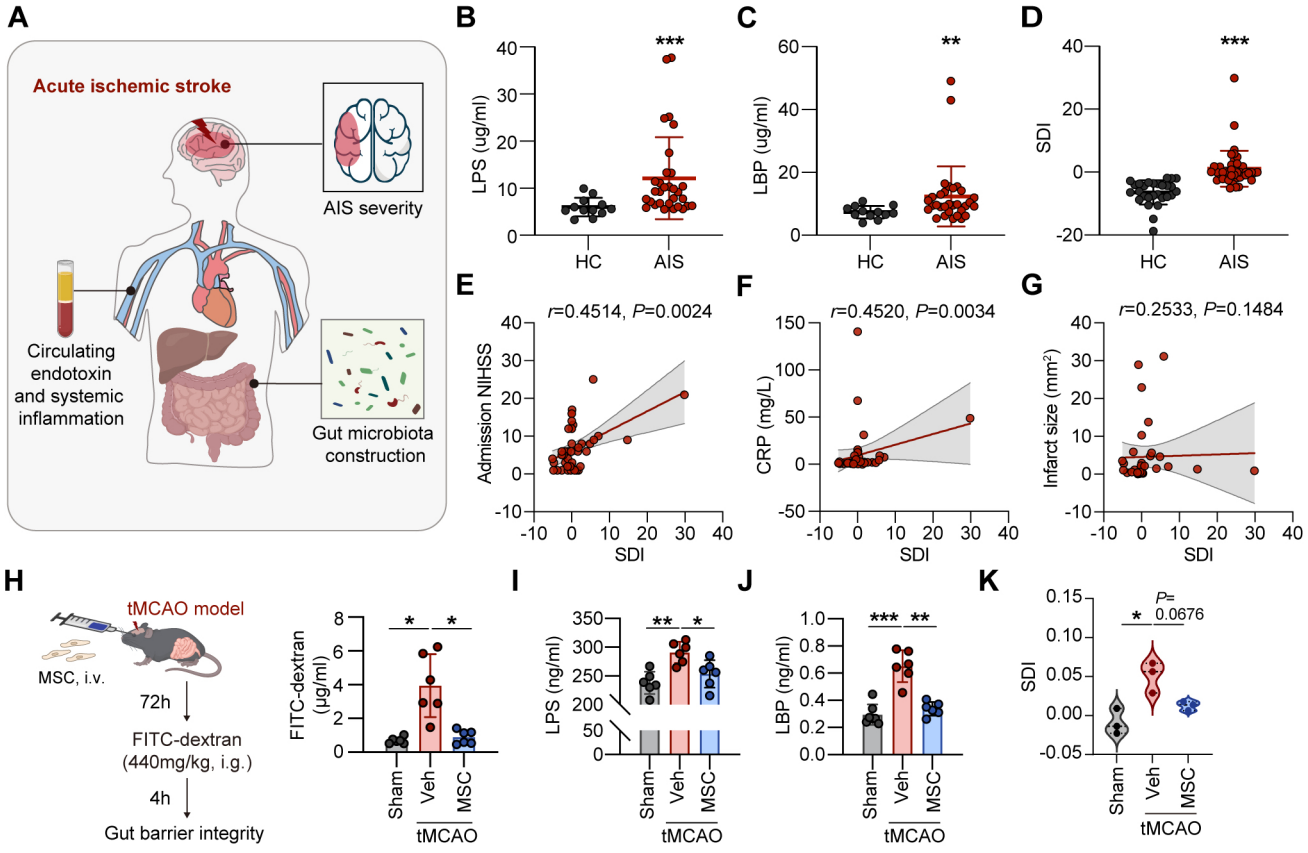

Figure 1 BM-MSC transfer ameliorates post-stroke enterobacterial translocation. (A) Experimental design of gut bacteria translocation in patients with AIS. Serum LPS (B) and LBP (C) level of patients with AIS (N=31) and HC (N=12) assessed by ELISA. *p<0.05, **p<0.01; by Welch's t-test (mean±SD). (D) Comparison of SDI in patients with AIS (N=43) and HC (N=28), ***p<0.001, by Welch's t-test (mean±SD). SDI of patients who had a stroke correlating with the admission NIHSS score (E), CRP level (F) and infarct size (G) in patients with AIS, by Spearman rank correlation test. (H–K) Wild-type C57/BL6 mice were subjected to 60 min of tMCAO and transferred with a single dose of BM-MSC (2×10^6 cells per mice, intravenous) or an equal volume of vehicle (Veh, intravenous) right after reperfusion. Serum and faecal samples were collected at 3 days after tMCAO. (H) Schematic diagram of the gut barrier integrity assay and the results of fluorescence quantification. N=6 in each group, *p<0.05, by Welch ANOVA (mean±SD). Serum LPS (I) and LBP (J) level of sham and stroke mice. N=6 mice in each group, *p<0.05, **p<0.01, ***p<0.001, by Welch ANOVA (mean±SD). (K) Comparison of SDI in sham and stroke mice. N=3 mice in each group, *p<0.05, by Welch ANOVA (mean±SD). AIS, acute ischaemic stroke; ANOVA, analysis of variance; BM-MSC, bone marrow-derived mesenchymal stem cell; CRP, C reactive protein; FITC, fluorescein isothiocyanate; HC, healthy control; LBP, lipopolysaccharides binding protein; LPS, lipopolysaccharides; NIHSS, National Institute of Health stroke scale; SDI, Stroke Dysbiosis Index; tMCAO, transient middle cerebral artery occlusion.

was positively correlated with NIHSS (National Institute of Health stroke scale) score in admission (figure 1E) and plasma C reactive protein level (figure 1F) in patients with AIS while seemed to be irrelevant to infarct size (figure 1G). The results revealed that enterobacterial dysbiosis of patients with AIS could affect neurological functions though the impact on lesion size was mild.

To explore the therapeutic effect of BM-MSC (online supplemental figure 2A–B) against post-stroke gut bacteria translocation, WT mice were subjected to 60 min of tMCAO and transferred with a single dose of BM-MSC (2×10^6 cells per mice, intravenous) or an equal volume of vehicle (Veh, intravenous) right after reperfusion (figure 1H–K). In accordance with previous reports, the BM-MSC recipients displayed ameliorated stroke severity with decreased infarct volume (online supplemental figure 3A–B), improved neurological function (online supplemental figure 3C–D) and increased post-stroke survival (online supplemental figure 3E). Accordingly, BM-MSC also improved the sensorimotor functions at 3–14 days after tMCAO (online supplemental figure 3F). To evaluate the gut barrier permeability of the stroke models, tMCAO mice were gavaged with fluorescein isothiocyanate-dextran (FITC-dextran; 3–5 kDa) at 3 days after stroke. Pronounced extravasation of FITC-dextran from the enteric cavity into the circulation was recorded in tMCAO models (figure 1H). As with patients with AIS, the stroke mice displayed increased LPS (figure 1I), LBP (figure 1J) and SDI (figure 1K). Increment of gut barrier permeability and bacterial products in the circulation revealed the enterobacterial translocation after stroke. Impressively, BM-MSC transfer downregulated FITC-dextran extravasation from the gut (figure 1H), serum LPS (figure 1I) and LBP (figure 1J) level and the SDI (figure 1K) indicating that the gut barrier integrity was preserved in the recipients and the enterobacterial translocation was inhibited. Our data suggested that besides improving stroke outcomes, BM-MSC treatment displayed promising therapeutic effects against post-stroke bacteria translocation.

BM-MSC transfer does not modulate the gut structure

As far as we are concerned, post-stroke enterobacterial translocation was dependent on three elements: Integrity of the gut structure, the thickness of mucus layer and construction of gut microbiota. To explore the mechanisms of how BM-MSC protect against post-stroke enterobacterial translocation, gut structure integrity was first assessed.

We documented that although the body weight of mice was decreased after stroke, it was not reversed by BM-MSC transfer (figure 2A). The length of the gut was comparable among sham-operated controls, Veh-treated and BM-MSC-treated tMCAO models (figure 2B) and the hierarchical structure was similar as assessed by HE staining (figure 2C). Bulk RNA sequencing (RNA-seq) with the colon tissue showed unaltered transcription of tight junction proteins between the stroke models with or without BM-MSC treatment (figure 2D) which was further confirmed by immunostaining of zona occludens 1 (figure 2E) and Claudin 4 (figure 2F) in colon epithelial cells. Therefore, we concluded that the protection against post-stroke enterobacterial translocation by BM-MSC transfer was independent of the modulation of the gut structure.

Colon mucus layer is attenuated after stroke which is preserved by BM-MSC transfer

We next explored the impacts of BM-MSC transfer on the colon mucus layer. Alcian blue staining revealed attenuation of the colon mucus layer and compression of the colon crypt (figure 3A,B) after stroke. Strikingly, BM-MSC transfer efficiently reversed the thickness of the mucus layer (figure 3A,B). Mucins are major constituent proteins of the mucus layer.[7 18] As revealed by RNA-seq with colon tissue, BM-MSC recipients showed upregulated mucin synthesis (figure 3C,D). Consistently, immunostaining (figure 3E) and ELISA (figure 3F) demonstrated the increased expression of Mucin-2 (MUC2) in the colon of BM-MSC-transferred mice. We thus inferred that inhibition of post-stroke enterobacterial translocation by BM-MSC transfer could be attributed to the preservation of the colon mucus layer.

BM-MSC improve gut microbiota construction through preserving colon mucus layer

We further evaluated the gut microbiota construction of tMCAO mice after BM-MSC treatment with 16S ribosomal RNA sequencing of faeces samples. Principal coordinate analysis (figure 4A) and unweighted pair group method with arithmetic mean analysis (figure 4B) revealed the alteration of gut microbiota construction after tMCAO which was reversed by BM-MSC treatment. BM-MSC upregulated the abundance of several probiotics including members of the phylum of Verrucomicrobiota and the subordinated species of *Akkermansia muciniphila* (figure 4C–F). Considering the mutual promotion of the mucus layer and *Akkermansia muciniphila*,[19–21] we sought to figure out the causal relationship between the improved colon mucus layer and the expanded *Akkermansia muciniphila* abundance in BM-MSC recipients. Gut microbiota was depleted with pretreatment of ABX for 28 days before tMCAO (figure 4G and online supplemental figure 4A–E). Interestingly, the neural protective effects of BM-MSC against AIS were unabolished by ABX (online supplemental figure 4A–D). Moreover, the preservation of gut barrier integrity was unaffected by ABX treatment in the BM-MSC recipients as evidenced by the improved thickness of colon mucus layer (figure 4H), the increased goblet cell count in the colon crypt (figure 4H) and the decreased extravasation of garaged FITC-dextran (figure 4I). These results illustrated that the reconstruction of gut microbiota by MSC transfer was attributed to the improved integrity of the colon mucus layer.

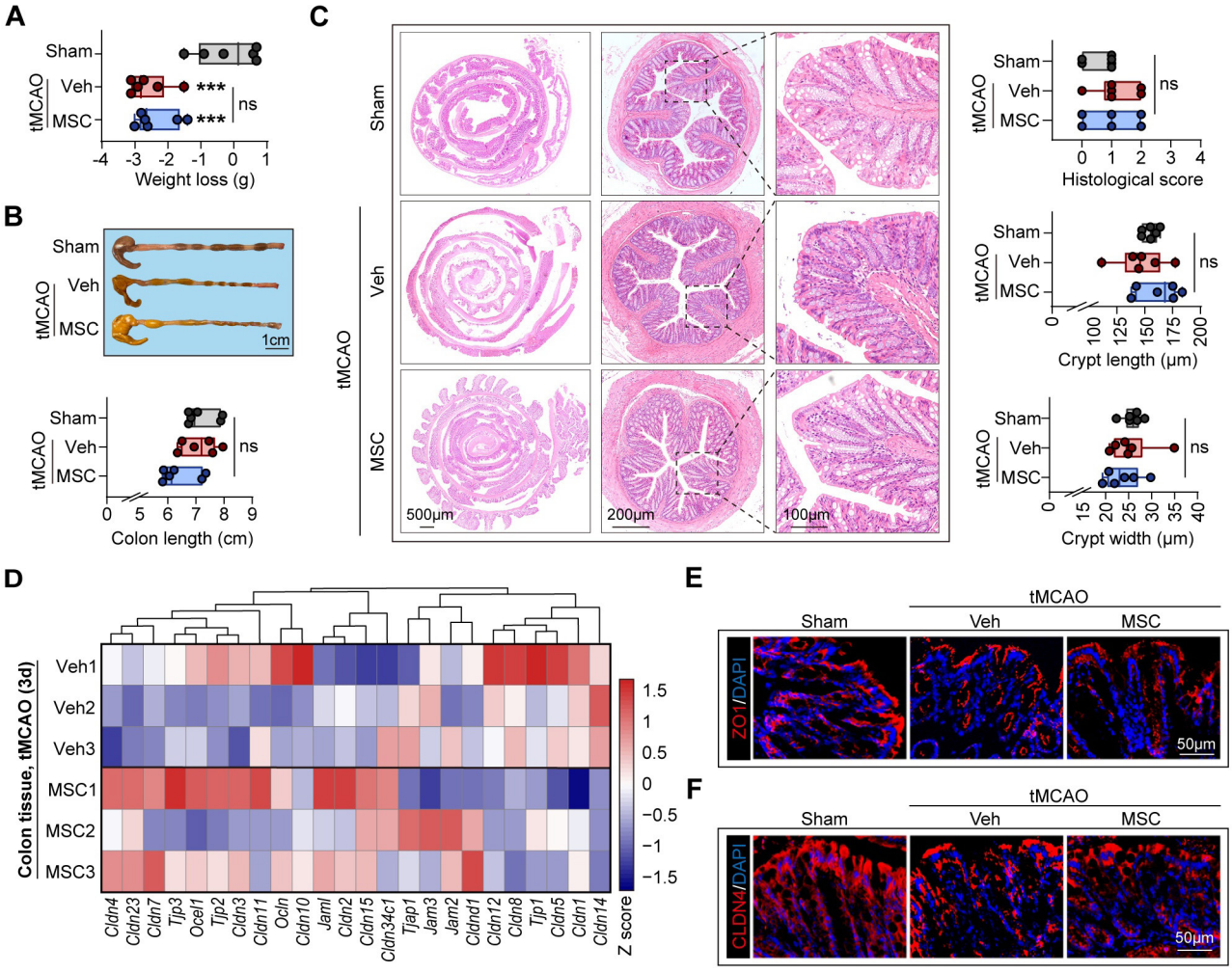

Figure 2 BM-MSC transfer does not modulate gut structure. (A) Weight loss (d3–d1) in mice of sham, tMCAO+Veh and tMCAO+MSC. N=6 mice in each group. ***p<0.001, compared with sham group. Not significant, by one-way ANOVA (mean±SD). (B) Representative picture of colon in sham, tMCAO+Veh and tMCAO+MSC mice and the quantification of colon length. N=6 mice in each group. Not significant, by one-way ANOVA (mean±SD). (C) Colon H&E stained and statistics of the histological score, crypt length and width in sham, tMCAO+Veh and tMCAO+MSC mice. N=6 mice in each group. Not significant, by one-way ANOVA (mean±SD). (D) Heatmap of tight junction-related genes of colon tissue between Veh and MSC after 3 days of tMCAO according to bulk RNA sequencing (RNA-seq), N=3 mice in each group. (E–F) Representative images of ZO1(E) and CLDN4 (F) of colon tissue in mice of in sham, tMCAO+Veh and tMCAO+MSC groups. N=3 mice in each group. ANOVA, analysis of variance; BM-MSC, bone marrow-derived mesenchymal stem cell; CLDN4, Claudin 4; tMCAO, transient middle cerebral artery occlusion; ZO1, zona occludens 1.

BM-MSC preserve gut barrier integrity through liver-gut axis

In AIS, activation of the hypothalamic-pituitary-adrenal (HPA) axis in response to the brain injury results in the elevation of systemic GCs. We verified the elevation of GCs in patients with AIS (online supplemental figure 5A). At 3 days after tMCAO, plasma cortisol concentration was pronouncedly upregulated in the stroke models which was ameliorated by BM-MSC transfer (figure 5A). Correspondingly, with bulk RNA-seq, we observed that steroid hormone biosynthesis was among the top 10 downregulated signalling pathways in BM-MSC-treated mice as assessed with Kyoto Encyclopedia of Genes and Genomes enrichment (figure 5B). To be noticed, DEX suppressed transcription (figure 5C) and translation (figure 5D–E) of MUC2 in goblet cells in dose-dependent manner with no significant effects on the cell survival (online supplemental figure 5B). When DEX was injected into BM-MSC recipients to reinforce the systemic GC level (online supplemental figure 5C), the protection against mucus layer attenuation by BM-MSC was abolished (figure 5F). Accordingly, DEX-treated BM-MSC recipients displayed increased infarct volume (online supplemental figure 5D), exacerbated gut barrier impairment (online supplemental figure 5E) which illustrated that BM-MSC preserved the mucus layer by inhibiting GC-dependent mucus injury.

The liver is the major organ responsible for GC catabolism. Hepatocytes express multiple enzymes to regulate the level and effects of GC. For example, HSD11B1 enforces the effects of GC while HSD11B2, CYP3A11,

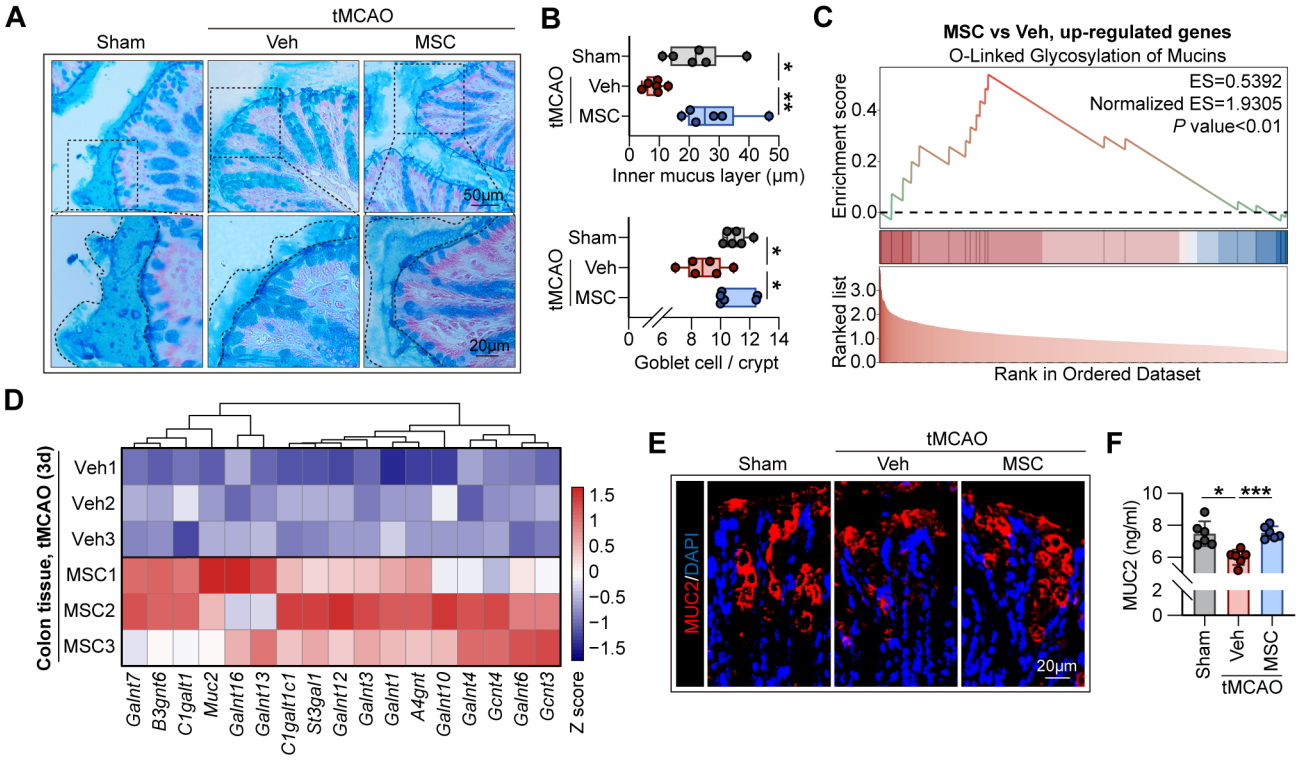

Figure 3 Colon mucus layer is attenuated after stroke which is preserved by BM-MSC transferred. (A–B) Alcian stain of colon tissue of sham, tMCAO+Veh and tMCAO+MSC mice. N=6 mice in each group. (A) Representative image of the mucus layer. (B) Corresponding quantitation of mucus layer thickness and number of goblet cells. Data were analysed using one-way ANOVA (mean±SD). *p<0.05, **p<0.01. (C–D) Analysis of sequencing results of colon tissue between tMCAO+Veh and tMCAO+MSC group. N=3 mice in each group. (C) GSEA showed that the upregulated genes in the MSC-treated group were enriched in the O-linked glycosylation of mucins pathway and the specific gene expression of this pathway was shown in the heatmap (D). (E) Immunostaining showed increased expression of MUC2 in the colon of BM-MSC-transferred mice. N=3 mice in each group. (F) Expression of colon MUC2 was quantified by ELISA. N=6 mice in each group. *p<0.05, ***p<0.001, by one-way ANOVA (mean±SD). ANOVA, analysis of variance; BM-MSC, bone marrow-derived mesenchymal stem cell; GSEA, gene set enrichment analysis; MUC2, Mucin-2; tMCAO, transient middle cerebral artery occlusion.

SRD5A1, SRD5A2 and AKR1D1 suppresses GC functions through accelerating its inactivation.[22–25] To be noticed, the transferred BM-MSC showed preferential infiltration into the liver but hardly stayed in the colon as revealed by optical in vivo imaging (figure 5G) and fluorescence microscopy (figure 5H). We thus hypothesised that liver functions were implicated in the mechanisms of BM-MSC-offered protection.

With the quantitative PCR array, we documented that the expression of *Hsd11b1* was increased while the transcription of GC inactivating enzymes including *Hsd11b2* and *Srd5a1* was declined in the liver at 3 days after tMCAO (figure 5I). Western blot (figure 5J) and immunostaining (figure 5K) revealed similar alteration of the proteins' expression illustrating that hepatocytes favoured enhancing GC effects after stroke. Notably, BM-MSC transfer reversed the upregulated expression of HSD1B1 and the decreased level of HSD11B2 and SRD5A1 (figure 5I–K). In consistence, bile acid analysis with targeted metabolomics showed that the metabolic status of the liver was similar between the BM-MSC recipients and sham-operated mice (online supplemental figure 6A,B). Meanwhile, RNA-seq with the liver tissue revealed that BM-MSC transfer enhanced steroids metabolism in hepatocytes (online supplemental figure 6C). Our data indicated that BM-MSC promoted GC inactivation by liver which subsequently preserved mucin production in the colon mucus layer.

BM-MSC accelerate GC inactivation through enhancing PPARγ signalling in hepatocytes

We next studied the underlying mechanisms of how BM-MSC promoted GC inactivation. A previous study reported that BM-MSC could modulated protein expression through epigenetic regulation.[26] The CpG island content of a gene tends to reflect the ease of its modification by methylation.[27] Nevertheless, we found that the predicted content of CpG island of *Hsd11b2* (online supplemental figure 7A) and the methylation of promoter and exon1 verified by bisulfite sequencing PCR analysis (online supplemental figure 7B) levels were all comparably low in the liver among the Sham-operated group, Veh-treated stroke mice and BM-MSC recipients. Similarly low CpG island content was predicted in the remaining genes (online supplemental figure 7C). Therefore, we

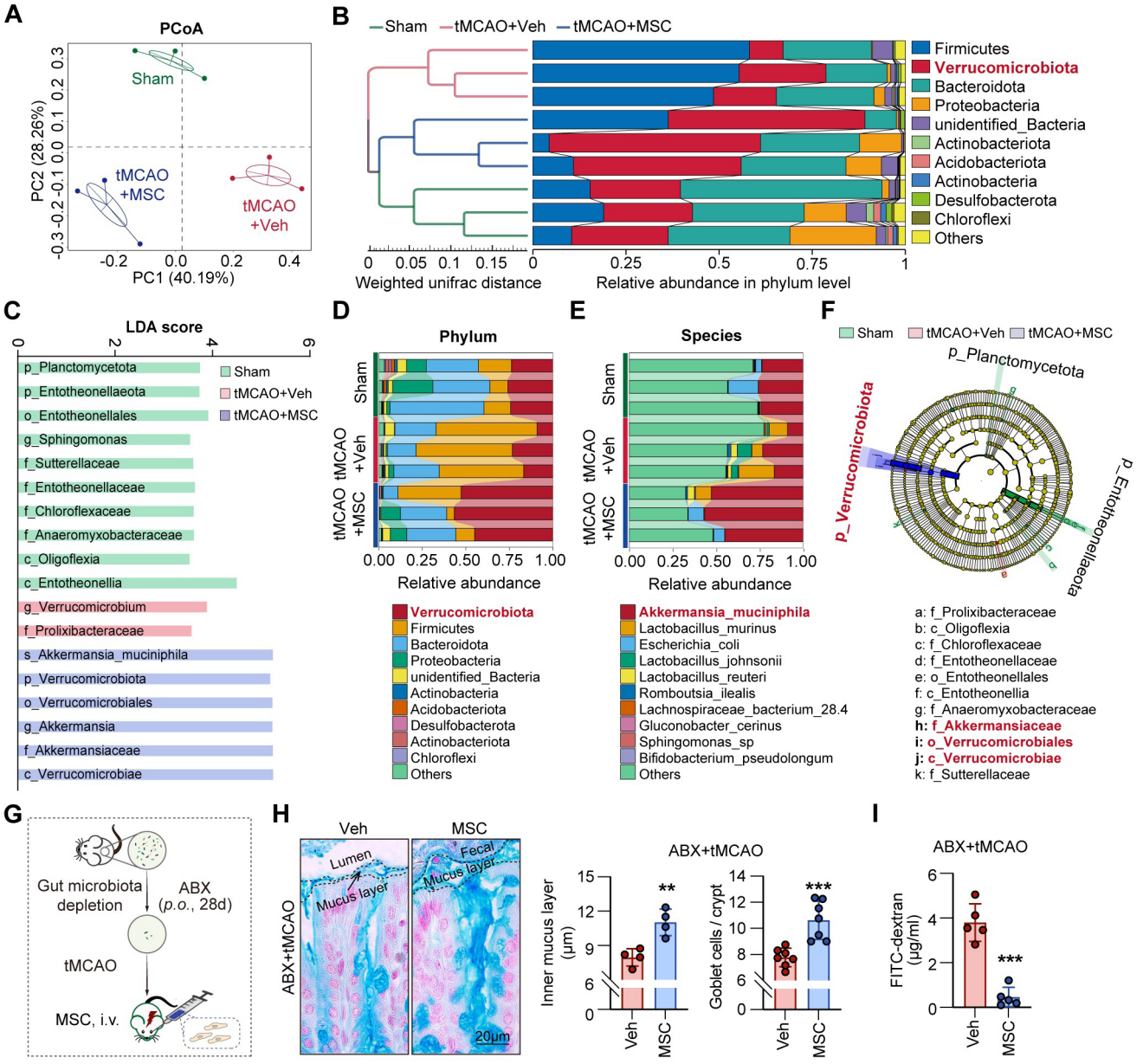

Figure 4 BM-MSC improves gut microbiota construction through preserving the colon mucus layer. (A–F) Faecal samples of mice at day 3 after tMCAO were collected and performed the 16S rRNA sequencing for the following analysis. N=3 mice in each group. (A) PCoA of the gut microbiome composition on the genus level. (B) Cluster analysis was performed using the unweighted pair group method with arithmetic mean (UPGMA) based on the weighted UniFrac distances to compare the community composition similarity of samples. (C) Characteristics of gut microbiota in the groups were evaluated with LEfSe. Bacterial populations with LDA score >3.5 were displayed. Relative abundance of gut bacterial phylum (D) and species (E) level in each group at day 3 after tMCAO. (F) Cladogram based on LEfSe analysis depicted the phylogenetic tree of the taxa enriched in microbiota from tMCAO mice received BM-MSC. (G–I) Gut microbiota was depleted with pretreatment of broad-spectrum antibiotics (ABX) for 28 days before tMCAO. (G) Experimental design. (H) Representative images of Alcian blue staining and statistics of mucus layer thickness showed that the repairing effect of BM-MSC on the mucus layer was inhibited by dexamethasone. N=4 mice of each group in the experiment measured the mucus layer, **p<0.01, by Student's t-test (mean±SD). N=7 mice in each group in the experiment measured the number of goblet cells. ***p<0.001, by Welch's t-test (mean±SD). (I) Gut barrier integrity was assessed as the results of fluorescence quantification of FITC-dextran. N=5 mice in each group, ***p<0.001, by Student's t-test (mean±SD). BM-MSC, bone marrow-derived mesenchymal stem cell; FITC, fluorescein isothiocyanate; LDA, linear discriminant analysis; LEfSe, linear discriminant analysis effect size; PCoA, principal coordinate analysis; rRNA, ribosomal RNA; tMCAO, transient middle cerebral artery occlusion.

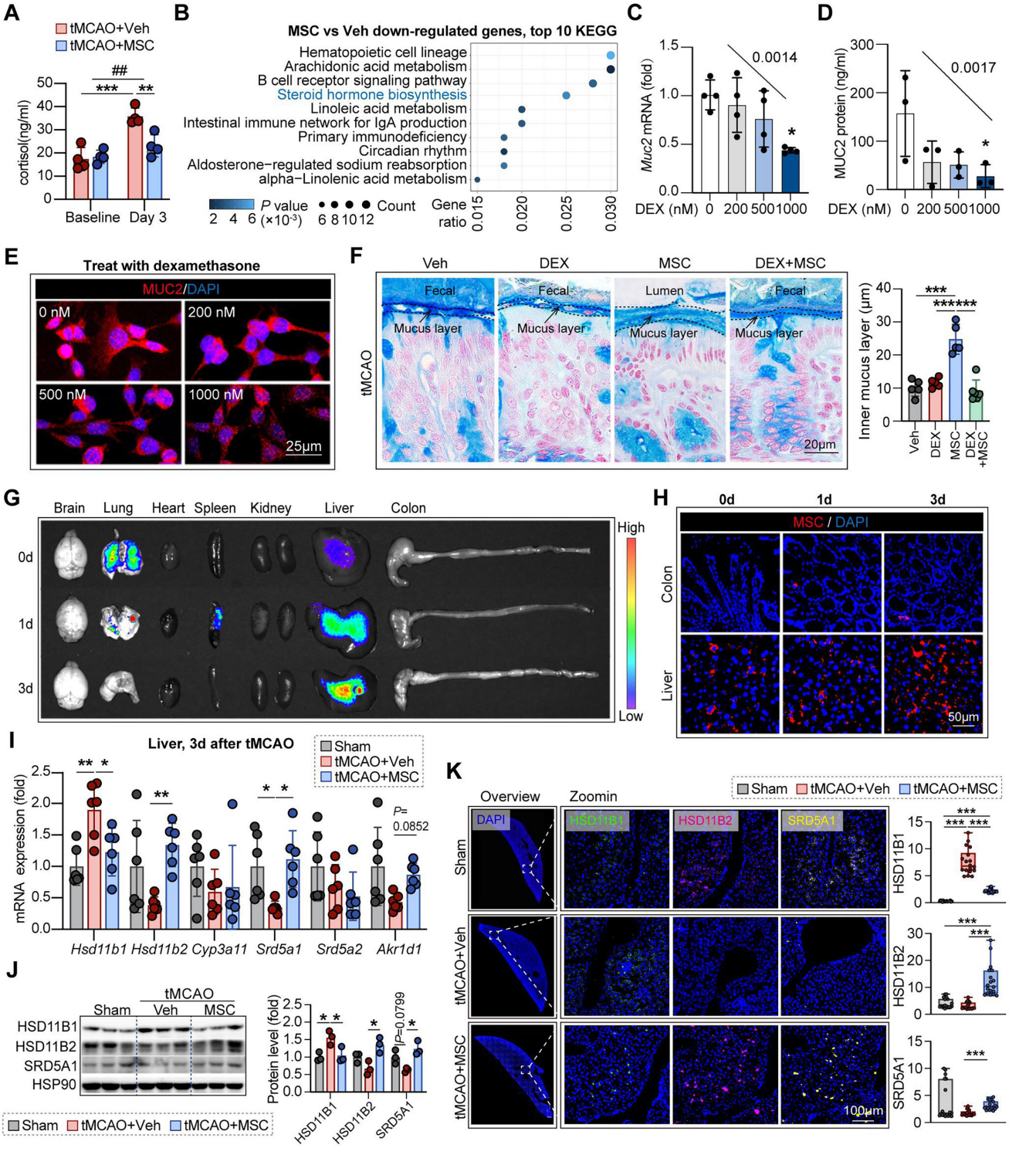

Figure 5 BM-MSC preserves gut barrier integrity through liver-gut axis. (A) Changes in plasma cortisol concentrations after stroke in mice. N=4 mice in each group. **p<0.01, ***p<0.001, comparisons were made between the two groups labelled. ##p<0.01 compared with baseline cortisol level in the whole experiment, by two-way ANOVA (mean±SD). (B) The differentially expressed genes down-regulated in the colons of BM-MSC treated group were enriched in the steroid hormone biosynthesis pathway. (C–E) To explore the inhibitory effect of glucocorticoid on the mucus layer, goblet cells were treated with a concentration gradient of dexamethasone for 18 hours. The transcription and translation of MUC2 were assessed by QPCR (C) and ELISA (D), respectively. Experiments were repeated for 3–4 times. *p<0.05, compared with the control group (0 nM), by one-way ANOVA (mean±SD). The slope of *Muc2* mRNA and MUC2 protein expression line treated with the concentration gradient dexamethasone were also calculated by simple linear regression. (E) Expression of MUC2 (red) of goblet cells after concentration gradients of dexamethasone treatment was assessed by immunofluorescence staining. Experiments were repeated for three times. In addition, the dexamethasone treatment at these concentrations did not accelerate apoptosis in goblet cells. Data were shown in online supplemental figure 5A. (F) Representative images of Alcian blue staining and statistics

of mucus layer thickness showed that the repairing effect of BM-MSC on the mucus layer was inhibited by dexamethasone. N=5 in each group. ***p<0.001, by one-way ANOVA (mean±SD). Additional data for dexamethasone treatment under these subgroups were presented in online supplemental figure B–D. (G) In vivo imaging of major organs from tMCAO mice at 0 day, 1 day and 3 days after intravenously injection of DiR-labelled BM-MSC (2×10^6 cells per mouse). N=3 mice in each group. (H) Infiltration of WGA-labelled BM-MSC of the liver and colon at 0 day, 1 day and 3 days after intravenously injection were tracked by immunofluorescence. N=3 mice in each group. (I–K) Liver tissue of stroke mice was isolated at 3 days after tMCAO and used for the following experiments. The expression of enzymes that regulated the level and effects of glucocorticoid were detected by QPCR array (I). N=6 mice in each group. *p<0.05, **p<0.01, by one-way ANOVA (mean±SD). The change of HSD11B1, HSD11B2 and SRD5A1 were further verified by Western blot (J) and immunostaining (K). N=3 mice in each group. *p<0.05, ***p<0.001, by one-way ANOVA (mean±SD). ANOVA, analysis of variance; BM-MSC, bone marrow-derived mesenchymal stem cell; DAPI, 4',6-diamidino-2-phenylindole; DEX, dexamethasone; IgA, immunoglobulin A; KEGG, Kyoto Encyclopedia of Genes and Genomes; mRNA, messenger RNA; MUC2, Mucin-2; QPCR, quantitative PCR; tMCAO, transient middle cerebral artery occlusion.

concluded that DNA methylation was independent of the GC metabolic regulation by BM-MSC.

Since we observed the opposite effects of BM-MSC on the expression of HSD11B1, HSD11B2 and SRD5A1 in the liver, we inferred that a common coordinator that regulated HSD11B1, HSD11B2 and SRD5A1 transcription was implicated in the therapeutic mechanism. Transcriptional factors (TFs) that downregulated HSD11B1 expression or upregulated HSD11B2 and SRD5A1 transcription were searched through the signalling pathways project. We found there are 64 TFs that could mediate the expression of all the three mentioned molecules (figure 6A). Among the 64 TFs, peroxisome proliferator-activated receptor γ (PPARγ) was the only TF that simultaneously suppressed HSD11B1 but promoted HSD11B2 and SRD5A1 transcription (figure 6A). With immunostaining (figure 6B), we documented that expression of PPARγ in the liver was suppressed after stroke which was rescued by BM-MSC transfer. After co-culture of BM-MSC with hepatocytes, PPARγ was observed to have translocation to the nucleus as assessed with immunostaining (figure 6C). An increased expression of *Pparg* was also detected in the hepatocytes (figure 6D). Simultaneously, BM-MSC downregulated *Hsd11b1* and increased the expression of *Hsd11b2* and *Srd5a1* in hepatocytes (figure 6D). These effects of BM-MSC were abolished when PPARγ signalling was inhibited by knocking down of *Pparg* in hepatocytes (figure 6E–F). Our results demonstrated that BM-MSC enhanced PPARγ signalling in hepatocytes thus promoted GC inactivation through coordination of HSD11B1, HSD11B2 and SRD5A1 expression. Therefore, the integrity of the colon mucus layer was preserved by BM-MSC treatment after cerebral ischaemic stroke.

DISCUSSION

The current study describes a previously unidentified alteration of the gut barrier after AIS. We find that systemic elevation of GCs induced by cerebral ischaemia leads to attenuation of the gut mucus layer which subsequently results in enterobacterial translocation. Transfer of BM-MSC preserves the gut barrier integrity and inhibits enterobacterial translocation through enhancing the metabolism of GCs by hepatocytes.

The perspective on stroke has evolved from a brain-centric view to a multi-organ viewpoint.[28 29] In consistent with previous studies, we recorded that the structure of serosal, muscular and submucous layer was intact in stroke models[6] while the thickness of the mucus layer was attenuated. The colonic mucus layer, as the main habitat for intestinal microorganisms, is mainly formed by mucin produced by goblet cells.[30 31] This study unveiled a delicate and sensitive change in the intestinal environment of the host after stroke. The loss of the mucus layer was the important reason for the post-stroke translocation of enterobacteria. Cerebral ischaemia provokes the HPA axis resulting in systemic elevation of GC level. Our data show that GC attenuates the productivity of mucin by goblet cells. Favourably, MSC treatment improves mucin production by goblet cells thus preserves the thickness of the gut mucus layer after stroke.

Besides the mucin production of goblet cells, the construction of gut microbiota contributes to the maintenance of the mucus layer.[32] Previous studies revealed that mucus components supported the survival of *Akkermansia muciniphila*.[33] In the meantime, *Akkermansia muciniphila* enhances mucin production and is thus beneficial for mucus preservation.[34] According to our results, the abundance of *Akkermansia muciniphila* was increased in the MSC-transferred stroke recipients. However, enrichment of *Akkermansia muciniphila* in the microbiota turned out to be a subsequent effect of improved mucus integrity in the MSC-recipients and was dispensable for the curative effects of MSC. Our findings emphasise the importance of host reaction in the protection offered by MSC while the improvement of gut microbiota composition is favourable side benefit.

In line with a previous study,[17] no significant correlation was found between SDI and infarct size, suggesting that the extent of infarction in the short term is mainly influenced by vascular factors. SDI serves as a quantitative measure reflecting the degree of gut dysbiosis in patients who had a stroke. The study indicates that SDI correlates with the NIHSS score suggesting a potentially significant role of the gut in influencing patient who had stroke outcomes. This underscores the need for further investigation into the relationship between gut dysbiosis and stroke prognosis.

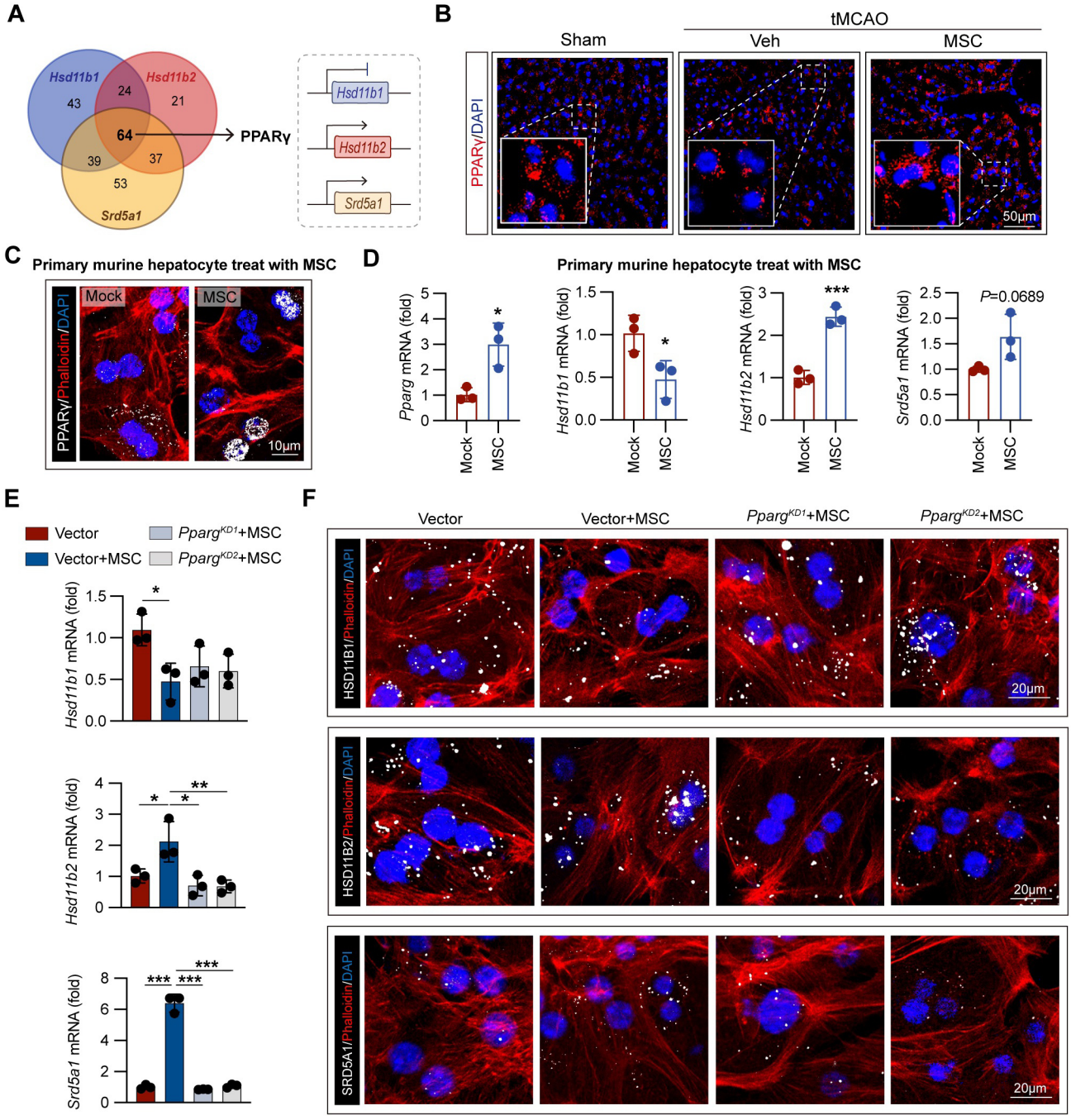

Figure 6 BM-MSC accelerates GC inactivation through enhancing PPARγ signalling in hepatocytes. (A) Venn diagram showed the intersection of TFs that modulated the transcription of *Hsd11b1*, *Hsd11b2* and *Srd5a1*. Among the 64 TFs intersected, PPARγ could simultaneously downregulated the transcription of *Hsd11b1* and upregulate the transcription of *Hsd11b2* and *Srd5a1*. Data for the analysis were obtained from the signalling pathways project (SPP, http://signalingpathways.org/). (B) Liver sections were subjected to immunostaining of PPARγ (red) and DAPI (blue) at 3 days after tMCAO. Experiments were repeated for three times. (C–D) Murine primary hepatocytes were co-cultured with BM-MSC (hepatocytes:BM-MSC=5:1) for 18 hours. (C) Immunofluorescence images showed enhanced nuclear localisation of PPARγ (grey) after co-culture of murine primary hepatocytes with BM-MSC. Experiments were repeated for three times. (D) The mRNA level of *Pparg*, *Hsd11b1*, *Hsd11b2* and *Srd5a1* in murine primary hepatocytes were assessed with QPCR. Experiments were repeated for three times. *p<0.05, ***p<0.001, by one-way ANOVA (mean±SD). (E–F) *Pparg* was knocked-down in murine primary hepatocytes by lentivirus-shRNA (*Pparg*^{KD}). Murine primary hepatocytes transfected with vector plasmid were set as control. The effect of *Pparg* in the promotion of glucocorticoid metabolism in hepatocytes by BM-MSC was verified by QPCR (E) and immunofluorescence (F). Experiments were repeated three times. *p<0.05, **p<0.01, ***p<0.001, by one-way ANOVA (mean±SD). ANOVA, analysis of variance; BM-MSC, bone marrow-derived mesenchymal stem cell; DAPI, 4‘,6-diamidino-2-phenylindole; mRNA, messenger RNA; PPARγ, peroxisome proliferator-activated receptor γ; QPCR, quantitative PCR; shRNA, short hairpin RNA; TFs, transcriptional factors; tMCAO, transient middle cerebral artery occlusion.

Intravenous infusion of MSC is a promising treatment for stroke.[8] As revealed by in vivo tracing, the transferred-BM-MSC favour infiltration into the liver rather than the gut. Interestingly, we demonstrate that it is the interaction of transferred-MSC and hepatocyte that mediates the mucus-preserving effects. We found that MSC enhanced GC metabolism in hepatocytes through increasing the expression of GC catabolic enzymes including HSD11B2. It has been recorded that the level of HSD11B2 in hepatocyte is regulated by DNA methylation[35] and Hedgehog signalling.[36 37] Nevertheless, the methylation status of the *Hsd11b2* gene and the activity of the Hedgehog pathway were both stable in the hepatocytes of the MSC recipients. Instead, MSC enhances the activation of PPARγ signalling, a key regulator of cellular metabolism, thus promoting the expression of HSD11B2 in hepatocytes and further improving mucin production by gut goblet cell. Our data suggest that the intravenously transferred-MSC synthetically protects against post-stroke enterobacterial translocation through coordinating systemic metabolism.

The present study has several limitations. First, the study used young mice whereas AIS commonly affects the elderly. Future research should include aged animal models to better reflect the clinical scenarios and evaluate age-specific treatment responses. Second, the experiments demonstrating that BM-MSC accelerates GC inactivation by enhancing PPARγ signalling in hepatocytes were all performed in vitro. Further in vivo studies are necessary to comprehensively elucidate the interactions and communications within these multi-organ systems.

Conclusively, we confirm that post-stroke MSC treatment improves gut barrier integrity and inhibits enterobacterial translocation by enhancing GC metabolism by hepatocytes. MSC transfer represents a protective modulator of the brain-liver-gut axis after AIS.

Acknowledgements The authors thank the Professor Andy Peng Xiang (Centre for Stem Cell Biology and Tissue Engineering, Key Laboratory for Stem Cells and Tissue Engineering, Ministry of Education, Sun Yat-sen University, Guangzhou, Guangdong, China) for technical support.

Contributors XS and TL contributed equally to the study. XS and TL designed and performed the experiments, collected and analysed the data and drafted the manuscript. YW contributed to the experimental design. LW contributed to the manuscript. BJ, XK and MH collected the clinical samples. CL collected the clinical data and revised the manuscript. SW and DL performed the animal experiments and collected the data. DL, XK, SS, HH, YL and XD collected the clinical data and revised the manuscript. BZ, WC and ZL designed and supervised the study and critically revised the manuscript. The authors read and approved the final manuscript. ZL is responsible for the overall content as guarantor.

Funding This work was supported by Guangzhou Key Research Program on Brain Science (202206060001 to ZL). Guangdong Basic and Applied Basic Research Foundation (2020A1515010056 to BZ). National Natural Science Foundation of China (82171307 to ZL). National Natural Science Foundation of China (82271348 to WC). Fundamental Research Funds for the Central Universities (23ykbj006 to WC). Science and Technology Program of Guangzhou (2023B01J1002 to ZL).

Competing interests None declared.

Patient consent for publication Not applicable.

Ethics approval Clinical research was approved by the ethics committee of the Third Affiliated Hospital of Sun Yat-sen University, China (approval no. RG2023-097-01). Participants gave informed consent to participate in the study before taking part.

Provenance and peer review Not commissioned; externally peer reviewed.

Data availability statement Data are available upon reasonable request. All data are available in the main text or the supplementary materials. Additional data related to this paper may be requested from the authors.

ORCID iDs
Wei Cai http://orcid.org/0000-0003-4059-4627
Zhengqi Lu http://orcid.org/0000-0002-2118-0368

REFERENCES

1 Owolabi MO, Thrift AG, Mahal A, *et al*. Primary stroke prevention worldwide: translating evidence into action. *Lancet Public Health* 2022;7:e74–85.
2 Stanley D, Mason LJ, Mackin KE, *et al*. Translocation and dissemination of commensal bacteria in post-stroke infection. *Nat Med* 2016;22:1277–84.
3 Xu K, Gao X, Xia G, *et al*. Rapid gut dysbiosis induced by stroke exacerbates brain infarction in turn. *Gut* 2021;70:1486–94.
4 Liu Q, Johnson EM, Lam RK, *et al*. Peripheral TREM1 responses to brain and intestinal immunogens amplify stroke severity. *Nat Immunol* 2019;20:1023–34.
5 Wen SW, Shim R, Ho L, *et al*. Advanced age promotes colonic dysfunction and gut-derived lung infection after stroke. *Aging Cell* 2019;18:e12980.
6 Oyama N, Winek K, Bäcker-Koduah P, *et al*. Exploratory Investigation of Intestinal Function and Bacterial Translocation After Focal Cerebral Ischemia in the Mouse. *Front Neurol* 2018;9:937.
7 Paone P, Cani PD. Mucus barrier, mucins and gut microbiota: the expected slimy partners? *Gut* 2020;69:2232–43.
8 Zhang W, Pu H, Hu X, *et al*. Poststroke Intravenous Transplantation of Human Mesenchymal Stem Cells Improves Brain Repair Dynamics and Functional Outcomes in Aged Mice. *Stroke* 2023;54:1088–98.
9 Wechsler LR, Bates D, Stroemer P, *et al*. Cell Therapy for Chronic Stroke. *Stroke* 2018;49:1066–74.
10 Kim D-W, Jeong H-S, Kim E, *et al*. Oral delivery of stem-cell-loaded hydrogel microcapsules restores gut inflammation and microbiota. *J Control Release* 2022;347:508–20.
11 Uccelli A, Laroni A, Freedman MS. Mesenchymal stem cells for the treatment of multiple sclerosis and other neurological diseases. *Lancet Neurol* 2011;10:649–56.
12 Shen Q, Huang Z, Yao J, *et al*. Extracellular vesicles-mediated interaction within intestinal microenvironment in inflammatory bowel disease. *J Adv Res* 2022;37:221–33.
13 Li T, Su X, Lu P, *et al*. Bone Marrow Mesenchymal Stem Cell-Derived Dermcidin-Containing Migrasomes enhance LC3-Associated Phagocytosis of Pulmonary Macrophages and Protect against Post-Stroke Pneumonia. *Adv Sci (Weinh)* 2023;10:2206432.
14 Zhang X, Huang W, Chen X, *et al*. CXCR5-Overexpressing Mesenchymal Stromal Cells Exhibit Enhanced Homing and Can Decrease Contact Hypersensitivity. *Mol Ther* 2017;25:1434–47.
15 Xu Y, Zhou Z, Kang X, *et al*. Mettl3-mediated mRNA m6A modification controls postnatal liver development by modulating the transcription factor Hnf4a. *Nat Commun* 2022;13:4555.
16 Cai W, Hu M, Li C, *et al*. FOXP3+ macrophage represses acute ischemic stroke-induced neural inflammation. *Autophagy* 2023;19:1144–63.
17 Xia G-H, You C, Gao X-X, *et al*. Stroke Dysbiosis Index (SDI) in Gut Microbiome Are Associated With Brain Injury and Prognosis of Stroke. *Front Neurol* 2019;10:397.

18 Nyström EEL, Martinez-Abad B, Arike L, *et al*. An intercrypt subpopulation of goblet cells is essential for colonic mucus barrier function. *Science* 2021;372:eabb1590.
19 van der Lugt B, van Beek AA, Aalvink S, *et al*. Akkermansia muciniphila ameliorates the age-related decline in colonic mucus thickness and attenuates immune activation in accelerated aging Ercc1−/Δ7 mice. *Immun Ageing* 2019;16:6.
20 Naama M, Telpaz S, Awad A, *et al*. Autophagy controls mucus secretion from intestinal goblet cells by alleviating ER stress. *Cell Host Microbe* 2023;31:433–46.
21 Alvarado DM, Chen B, Iticovici M, *et al*. Epithelial Indoleamine 2,3-Dioxygenase 1 Modulates Aryl Hydrocarbon Receptor and Notch Signaling to Increase Differentiation of Secretory Cells and Alter Mucus-Associated Microbiota. *Gastroenterology* 2019;157:1093–108.
22 Martins Nascentes Melo L, Herrera-Rios D, Hinze D, *et al*. Glucocorticoid activation by HSD11B1 limits T cell-driven interferon signaling and response to PD-1 blockade in melanoma. *J Immunother Cancer* 2023;11:e004150.
23 Boonen E, Vervenne H, Meersseman P, *et al*. Reduced cortisol metabolism during critical illness. *N Engl J Med* 2013;368:1477–88.
24 Nikolaou N, Gathercole LL, Kirkwood L, *et al*. AKR1D1 regulates glucocorticoid availability and glucocorticoid receptor activation in human hepatoma cells. *J Steroid Biochem Mol Biol* 2019;189:218–27.
25 Livingstone DEW, Di Rollo EM, Yang C, *et al*. Relative adrenal insufficiency in mice deficient in 5α-reductase 1. *J Endocrinol* 2014;222:257–66.
26 Liu S, Liu D, Chen C, *et al*. MSC Transplantation Improves Osteopenia via Epigenetic Regulation of Notch Signaling in Lupus. *Cell Metab* 2015;22:606–18.
27 Wang Q, Liang N, Yang T, *et al*. DNMT1-mediated methylation of BEX1 regulates stemness and tumorigenicity in liver cancer. *J Hepatol* 2021;75:1142–53.
28 Banerjee A, Mohapatra S, McCullough LD. Stroke and the Microbiome. *Stroke* 2024;55:762–4.
29 Honarpisheh P, Bryan RM, McCullough LD. Aging Microbiota-Gut-Brain Axis in Stroke Risk and Outcome. *Circ Res* 2022;130:1112–44.
30 Hansson GC. Mucins and the Microbiome. *Annu Rev Biochem* 2020;89:769–93.
31 Yang D, Jacobson A, Meerschaert KA, *et al*. Nociceptor neurons direct goblet cells via a CGRP-RAMP1 axis to drive mucus production and gut barrier protection. *Cell* 2022;185:4190–205.
32 Yao Y, Kim G, Shafer S, *et al*. Mucus sialylation determines intestinal host-commensal homeostasis. *Cell* 2022;185:1172–88.
33 Cani PD, Depommier C, Derrien M, *et al*. Akkermansia muciniphila: paradigm for next-generation beneficial microorganisms. *Nat Rev Gastroenterol Hepatol* 2022;19:625–37.
34 Shuoker B, Pichler MJ, Jin C, *et al*. Sialidases and fucosidases of Akkermansia muciniphila are crucial for growth on mucin and nutrient sharing with mucus-associated gut bacteria. *Nat Commun* 2023;14:1833.
35 Takaya J, Iharada A, Okihana H, *et al*. Magnesium deficiency in pregnant rats alters methylation of specific cytosines in the hepatic hydroxysteroid dehydrogenase-2 promoter of the offspring. *Epigenetics* 2011;6:573–8.
36 Zhu H, Zou C, Fan X, *et al*. Up-regulation of 11β-Hydroxysteroid Dehydrogenase Type 2 Expression by Hedgehog Ligand Contributes to the Conversion of Cortisol Into Cortisone. *Endocrinology* 2016;157:3529–39.
37 Daggubati V, Hochstelter J, Bommireddy A, *et al*. Smoothened-activating lipids drive resistance to CDK4/6 inhibition in Hedgehog-associated medulloblastoma cells and preclinical models. *J Clin Invest* 2021;131:e141171.